ROCK DISTRIBUTIONS AT THE INSIGHT LANDING SITE AND IMPLICATIONS FROM FRAGMENTATION THEORY. C. Charalambous[1], M. Golombek[2], T. Pike[1], N. H. Warner[3], C. Weitz[4], V. Ansan[5], E. Hauber[6], J. Grant[7], N. Williams[2], S. Wilson[7], A. DeMott[3], M. Kopp[3], H. Lethcoe[2]. [1]Imperial College, London, Department of Electrical and Electronic Engineering [2]Jet Propulsion Laboratory, California Institute of Technology, Pasadena, CA, [3]SUNY Geneseo, NY, Planetary Science Institute, [5]University of Nantes, Laboratory of Planetary and Geodynamics, [6]German Aerospace Center (DLR), [7]Center for Earth and Planetary Studies, National Air and Space Museum, Smithsonian Institution.

Introduction: The Discovery mission InSight (Interior Exploration using Seismic Investigations, Geodesy and Heat Transport) successfully landed in western Elysium Planitia on November 26, 2018. Dedicated to the study of the martian interior, the lander is located at 4.502°N/135.623°E (planetocentric coordinates) within a quasi-circular, shallow depression now known as Homestead hollow [1]. This is a heavily modified and degraded crater, with a smooth surface. Rock populations near the lander are mostly pebble sized with few large rocks. Beyond the hollow, more cobble and boulder size rocks are present.

In this work, we analyze the rock population statistics of areas nearby the lander by using images from both the lander-mounted Instrument Context Camera (ICC) and the robotic arm-mounted Instrument Deployment Camera (IDC).

Measurements: Measuring rocks in the workspace of InSight is required because the instruments must be deployed at locations free of 3 cm high rocks. Rock counts were measured multiple times by more than one person to check for consistency. Measurements were done separately through ArcGIS by fitting convex hulls and ImageJ by fitting ellipses. The diameter was taken as the average of the two horizontal axes.

Four main areas were identified for characterizing the rock abundance (Fig. 1): 1) a high rock abundance area to the west of the workspace, 2) the low rock abundance workspace area, 3) the instrument footprints, and 4) the far-field radiometer (RAD) spot on the rougher and rockier terrain to the northwest of the lander.

Fragmentation Theory: Based on the probabilistic calculation of the repeated fracture of a particle population, the model developed by Charalambous [2] allows an understanding of the time-dependent processes that formed the observed rock populations. These are described by a negative binomial (NB) function - a model which was applied to rock abundance predictions measured in HiRISE images of the InSight landing site [3]. The size distribution evolves over time at different rates according to the maturity index *t*. For the larger fragments on Mars, this parameter is determined by the number of meteorite impacts at the landing site constrained by saturation equilibria of the cratering production functions [4] and the age of the surface [3].

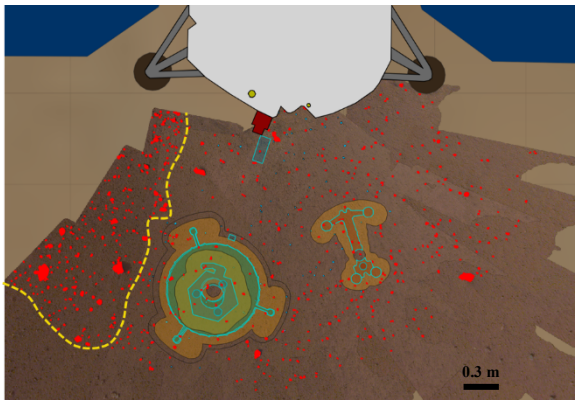

Figure 1. InSight WebGIS image of workspace near the lander (top). The yellow dashed line indicates the high rock abundance area which is a transition between the smooth inner hollow plains and the disturbed field from the retrorockets. Manually counted rocks larger than 1 cm are shown in red.

Size-Frequency Distributions: The cumulative fractional area (CFA) covered by rocks versus diameter is shown in Figure 2. In three of the areas, rocks greater than 5 cm diameter have distributions that fall between 1% and 4% area covered by rocks in exponential rock size-frequency models that have been used to describe rock populations for landing spacecraft [5, 6]. Measuring just the larger rocks (10-30 cm) at the edge of the workspace yields a CFA close to an exponential model rock abundance of 1-2%, which is close to the rock abundance at the Phoenix landing site [6]. At diameters below 5 cm, the CFA increases steeply approaching 9% CFA for rocks >1 cm and most closely resemble clast counts on the Gusev cratered plains from Spirit [5].

The equivalent plot in cumulative number of rocks per square meter versus diameter is shown in Figure 3. The distributions exhibit very steep slopes for diameters below 5 cm and for larger diameters, the size-frequency distributions have slopes that are similar to the exponential model distributions for CFAs of 1-10%. For the largest rocks with diameters 10-20 cm, the size-frequency distributions are consistent with a rock abundance of 1-2%. At diameters smaller than 4 cm, the slope of the distributions is steeper than the exponential models and similar to clast counts on the Gusev cratered plains [5]. Taken together, these rock distributions and CFAs are similar to the 1-3% measured at the Phoenix

landing site [6] and below the 5-7% at the Spirit landing site [5] for diameters >10 cm.

Figure 4 shows the cumulative number versus diameter counts compared with NB fits to the Phoenix and Spirit landing sites. The InSight rock distributions are most similar to the Phoenix landing site and less than the Spirit landing site.

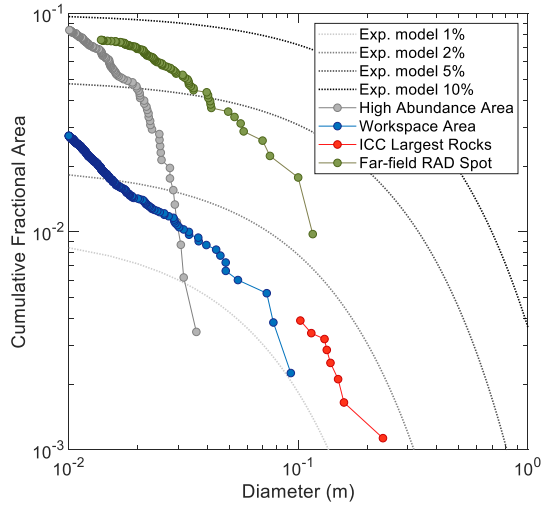

Figure 2 Cumulative Fractional Area (CFA) of rocks versus diameter within the near vicinity of the IDC high resolution mosaic, workspace area and RAD spot. Dotted lines are 1%, 2%, 5% and 10% exponential models [6].

This is consistent with expectations from average rock statistics of the entire landing E9 ellipse (130 km by 27 km) [3]. The low rock abundance within the hollow is due to dearth of rocks larger than 10 cm, as indicated by the higher rock abundance found from larger rocks >10 cm present in the far field.

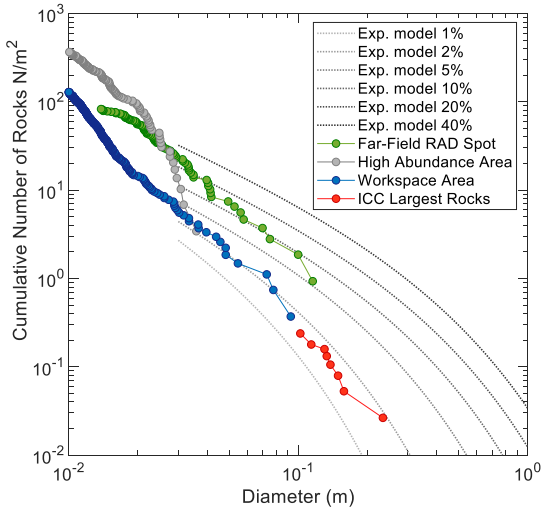

Figure 3 Cumulative number of rocks versus diameter per square meter with 1%, 2%, 5%, 10%, 20% and 40% exponential models cropped at 3 cm.

The InSight rock distribution fits an estimated maturity index of $t = 2.8 \pm 0.3$ (Figure 4), consistent with the Hesperian surface age of the E9 landing ellipse. Given the NB statistics, the observed population is therefore estimated to be the product of ~3 impacts on average. Between 1 – 4 cm, the workspace area distribution decreases relative to the higher rock abundance area, the model and the Phoenix NB fit. This decrease in the distribution in the hollow is likely due to the pebbles and sand that were deposited in the crater as it degraded [8]. The higher abundance area shows the transition to a rockier field to the west of the lander [8], possibly mixed with the disturbed field of duricrust fragments [9]. The derived NB fit from 30 cm to sub-cm appears as the interplay between these two distributions.

Due to the inherent multiplicity effect of the NB statistics (here at $t = 2.8$), the extrapolation of the NB fit to 1 mm (Figure 4) and similarly down to an upper limit for saltating grains [10], indicates an overall population rich in sand-sized material, consistent with orbital thermal inertia measurements [3] and the low rock abundance at the landing site.

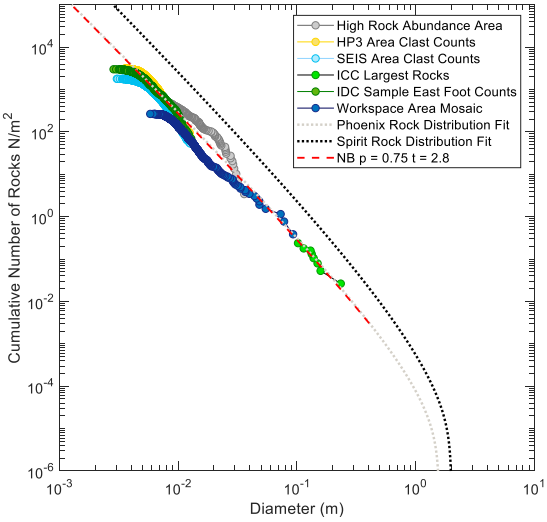

Figure 4 Cumulative number of rocks per meter squared versus diameter including sub-cm clast observations within each instrument foot-print area [7]. For comparison, the dotted lines depict Spirit and Phoenix fits to the NB fragmentation model [3], with the red dashed line the NB fit to InSight.

References: [1] Parker, T. *et al.* (2019) this issue. [2] Charalambous (2014) PhD Thesis, ICL. [3] Golombek, M., *et al.* (2017) *SSR*, 211, 5-95. [4] Hartman, W. (2005) *Icarus* 174, 294–320. [5] Golombek *et al.* (2006) *JGR,* 211. [6] Golombek *et al.*, (2012), *Mars* 7, 1-22. [7] Weitz *et al.* (2019) this issue. [8] Warner *et al.* (2019) this issue. [9] Ansan *et al.* (2019), this issue. [10] Golombek et al. (2018) 49th *LPSC,* #2319.